SUMMARY OF INFORMATION ON AIR INLETS

NACA SUBMERGED INLETS

By Emmet A. Mossman

Ames Aeronautical Laboratory

Selecting a type of air inlet suitable for a high-speed airplane is no longer a question merely of obtaining optimum pressure recovery, or of structural or arrangement desirability. Air inlets are becoming a principal factor in determining the fuselage size and shape, which in turn directly affect the airplane drag. The increased importance of fuselage drag in the transonic speed range has been pointed out by Schamberg in reference 1.

Submerged inlets have been shown to be practicable at high subsonic speeds for certain engine installations. (See references 2, 3, and 4.) An example of this is the Republic Aviation Corporation's modification of an F-84 Thunderjet airplane in which the installation of a radar nose was made possible by substitution of submerged inlets for the conventional nose inlet. The installation is shown in figure 1. This change was reportedly accomplished with no loss in airplane performance. However, knowledge of the characteristics of these and other inlets at transonic speeds is rather meager. This lack of information has been the result of the limitations of testing facilities in this speed range, and of the higher priority of other research. Investigations are now under way of the inlet types thought to be most promising. The data presented in this paper summarize the recent results of research at transonic speeds on NACA submerged inlets. Three transonic testing techniques were used: the wind-tunnel transonic bump, the flight wing-flow method, and a small high-speed wind tunnel.

The NACA divergent-wall submerged inlet has been investigated on a transonic bump in the Ames 16-foot high-speed tunnel. A schematic view of the bump mounted in the wind tunnel, with the submerged inlet installed, is shown in figure 2. Angle of attack for side-inlet installations was simulated by angular changes of the model in the plane of the bump surface. The pressure-recovery measurements were taken by 30 total-pressure tubes in six rows just behind the duct lip, and the pressure recoveries shown are the weighted averages of these measurements.

Some results of the transonic-bump investigation are shown in figure 3 for a duct having a width-depth ratio of 4.0 ($W/d = 4$). The ordinate for these curves is ram-recovery ratio, which is the ratio of the ram pressure recovered to the ram pressure available. It may be

seen that there was a gradual but slight decrease in pressure recovery in the Mach number range from 0.9 to 1.1 for mass-flow ratios of 0.35, 0.45, and 0.55, where mass-flow ratio is defined as the ratio of the mass of air flowing into the inlet M_1 to the mass of air flowing through an equal area in the free stream M_0. The pressure recovery was increasing again at the highest free-stream Mach number of 1.15. The effect on the pressure recovery of changes in angle of attack for angles up to 8° was found to be slight within the range of these tests. In some cases, increasing the angle of attack was beneficial to the pressure recovery. These data are believed to indicate the trend that may be expected in the transonic speed range with this type of inlet. However, the ram-recovery ratios obtained with this arrangement, while useful qualitatively, should not be construed as a precise indication of the true entrance pressure loss to be expected on a full-scale airplane. The severe flow angularity in the corner regions of the duct entrance, the low mass-flow ratios, and the thickness of the transonic-bump boundary layer make precise measurement difficult. The effect on the pressure recovery of the boundary layer into which the inlet was placed is shown in figure 4. The abscissa is a boundary-layer parameter h/d representing the ram defect of the boundary layer at the inlet position $\left[\frac{h}{d} = \frac{1}{d}\int_0^{\delta} \frac{\Delta H}{H_0 - p_0}\, dy, \text{ (reference 5)}\right]$ where

ΔH loss in total pressure in the boundary layer

$H_0 - p_0$ free-stream ram pressure

d depth of the duct

δ boundary-layer thickness

Larger boundary-layer losses are represented by larger values of h/d. The pressure loss in the boundary layer, as indicated by h/d, can be seen to be greater for the transonic bump than was observed in a previously reported test of a $\frac{1}{4}$-scale model of a fighter airplane.

The effect of this thicker boundary layer on the pressure recovery in the inlet is seen to be of large magnitude. For comparable Mach numbers and mass-flow ratios the values of ram-recovery ratios are approximately 0.84 for the transonic-bump investigation and 0.92 for the $\frac{1}{4}$-scale airplane model installation. Mach number distributions along the ramp center line corresponding to free-stream Mach numbers of 0.74, 1.02, and 1.15 are shown in figure 5. A shock formation was

evidenced at about 60 percent of the ramp length at a Mach number of 1.02. As the free-stream Mach number was increased, the shock became stronger and moved downstream slightly. These tests will be extended, and data for higher mass-flow ratios will be obtained.

Although test data from the transonic bump indicate no adverse effects on the pressure recovery at transonic speeds, exploratory tests in flight utilizing the wing-flow technique showed that the operation of the inlet at transonic speeds is critical to changes in inlet geometry. In this investigation the pressure gradient down the ramp was more unfavorable than in the bump tests because of an increase in the width to depth ratio of the entrance. Separation due to boundary-layer shock-wave interaction did occur at transonic speeds for mass-flow ratios below 0.4.

The ability of the divergent-wall inlet to operate with satisfactory pressure recovery at free-stream Mach numbers somewhat greater than 1.0 has been attributed to the thinness of the boundary layer along the inlet ramp. A comparison of the boundary-layer growth on parallel-wall and divergent-wall ramps is shown in figure 6 for a mass-flow ratio of 0.6. Here the momentum thickness down the center line of the ramp is given from measurements and from theoretical calculations by use of the known pressure distributions. It may be seen from this figure that the growth of the boundary layer in the divergent-wall inlet, as experimentally measured at low speeds, is approximated theoretically by assuming a three-dimensional growth (reference 6) which allows for thinning of the boundary layer due to lateral motion. The agreement between the measured boundary-layer growth and the growth calculated by theory for the parallel-wall inlet is shown by the two upper plots. The boundary-layer momentum thickness for the divergent-wall inlet can be seen to have been much thinner than for the parallel-wall inlet. Research on the interaction of boundary layers with shock waves has shown that a thin boundary layer does not separate as readily in the presence of a shock wave as does a thicker boundary layer. In the transonic-bump investigation, the interaction of the ramp shock wave with the ramp boundary layer did not become severe enough to cause separation along the ramp of the divergent-wall inlet. Thus, the relatively thin ramp boundary layer of the NACA submerged inlet enhances both the subsonic and the transonic operation of the inlet.

Of course, during subsonic operation at mass-flow ratios above 0.4, the pressure losses due to the boundary layer in the divergent-wall inlet are not the principal pressure losses. In the absence of boundary-layer separation, the main part of the pressure losses of an NACA submerged inlet is in the turbulent mixing regions which originate along the side walls of the ramp (reference 7). It has been shown that these loss regions are actually rolled-up vortex sheets generated along the outside edges of the divergent walls. Flow pictures were obtained by

[redacted]

plunging a small model of the submerged inlet into a tank of water which had aluminum powder sprinkled on the surface. (See fig. 7.) The model was mounted on a rack and lowered into the water. The resulting vortex formation from the oblique side walls (fig. 8) is shown in the two regions indicated by the broad arrows. The effect of the passing of these vortex regions through the oblique shock wave on the ramp is not known, but the results of the transonic-bump tests in the Ames 16-foot high-speed tunnel indicate that it was not adverse. Successful transonic operation of the submerged inlet is believed to be a function of the intensity of the interaction between the ramp boundary layer and the shock wave.

It has been suggested that boundary-layer control be utilized to delay the onset of shock-wave induced separation. Tests were made at low speeds of a large-scale model of an NACA submerged inlet in which the rearward 45 percent of the inlet ramp was constructed of porous bronze material. The model of the air-induction system was mounted on a dummy wall of an Ames 7- by 10-foot tunnel. The tunnel boundary layer passed beneath the dummy wall. Measurements were made in the duct by a rake of 90 total-pressure tubes. Some preliminary results of these tests are shown in figure 9. Removal of the ramp boundary layer had the greatest effect at the low mass-flow ratios. According to an analysis which is to be presented by Norman J. Martin in a subsequent paper, instability of twin-inlet operation should be almost eliminated with a suction mass-flow ratio of 0.06. The ramp boundary layer at the end of the porous plate was almost completely eliminated for the conditions shown in figure 9. It should be noted that the quantity of air removed through the porous plate and the estimated power required for removal of this air is small. These results are from low-speed tests, however, and the efficacy of removing the ramp boundary layer through a porous surface at transonic speeds and thus extending satisfactory inlet operation has not yet been proven. Preliminary tests at transonic speeds of a simulated NACA submerged inlet in a small wind tunnel have shown no separation of the ramp boundary layer at free-stream Mach numbers of approximately 1.15. These results are similar to those obtained in the Ames 16-foot high-speed tunnel. Thus, since boundary-layer separation induced by shock formation was not encountered, porous suction had no noticeable effect when applied in the small-wind-tunnel test.

The results presented in this paper indicate that the pressure recovery characteristics of NACA submerged inlets at transonic speeds are promising; however, the data are as yet incomplete, and further research is needed.

REFERENCES

1. Schamberg, R.: Effects of Flight Speed and Propulsive System on Aircraft Range. Rep. R-114, Rand Corp., Aug. 13, 1948.

2. Hall, Charles F., and Barclay, F. Dorn: An Experimental Investigation of NACA Submerged Inlets at High Subsonic Speeds. I - Inlets Forward of the Wing Leading Edge. NACA RM A8B16, 1948.

3. Hall, Charles F., and Frank, Joseph L.: Ram-Recovery Characteristics of NACA Submerged Inlets at High Subsonic Speeds. NACA RM A8I29, 1948.

4. Anon.: All-Weather Thunderjet. Aviation Week, vol. 51, no. 2, July 11, 1949, p. 14.

5. Mossman, Emmet A., and Randall, Lauros M.: An Experimental Investigation of the Design Variables for NACA Submerged Duct Entrances. NACA RM A7I30, 1947.

6. Kehl, A.: Investigations on Convergent and Divergent Turbulent Boundary Layers. R.T.P. Translation No. 2035, British Ministry of Aircraft Production. (From Ingenieur Archiv. Vol. XIII, No. 5, 1943, pp. 293-329.)

7. Delany, Noel K.: An Investigation of Submerged Air Inlets on a 1/4-Scale Model of a Typical Fighter-Type Airplane. NACA RM A8A20, 1948.

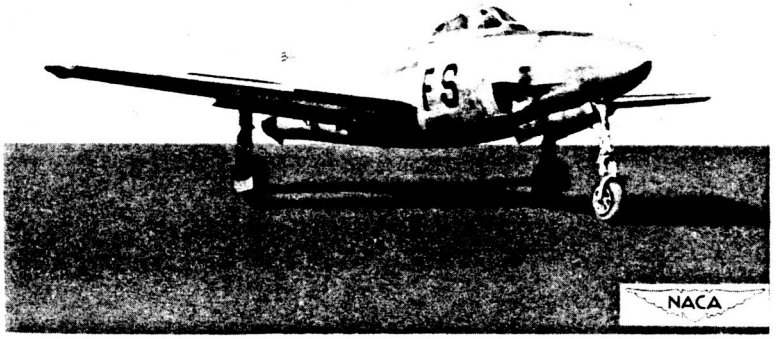

Figure 1.- The Republic F-84 with NACA submerged inlets.

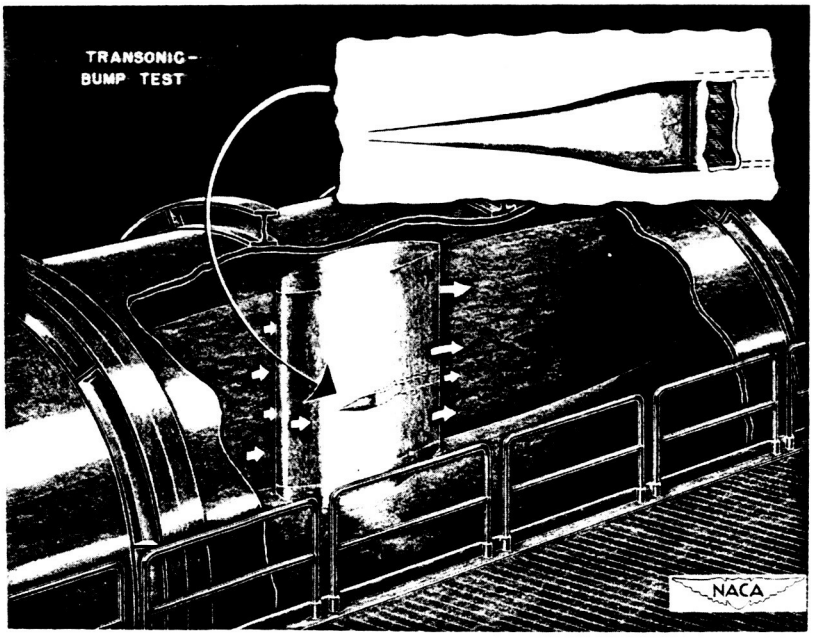

Figure 2.- The transonic-bump installation in the Ames 16-foot high-speed tunnel.

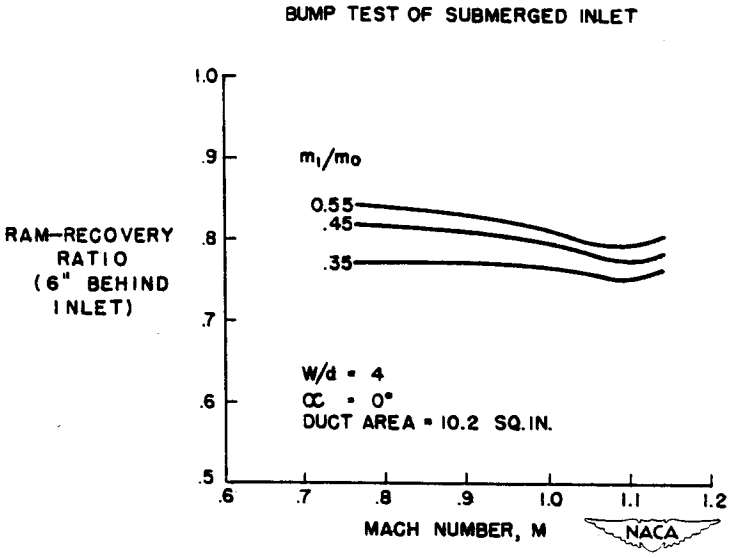

Figure 3.- Effect of Mach number on the ram-recovery ratio from the transonic-bump tests of an NACA submerged inlet.

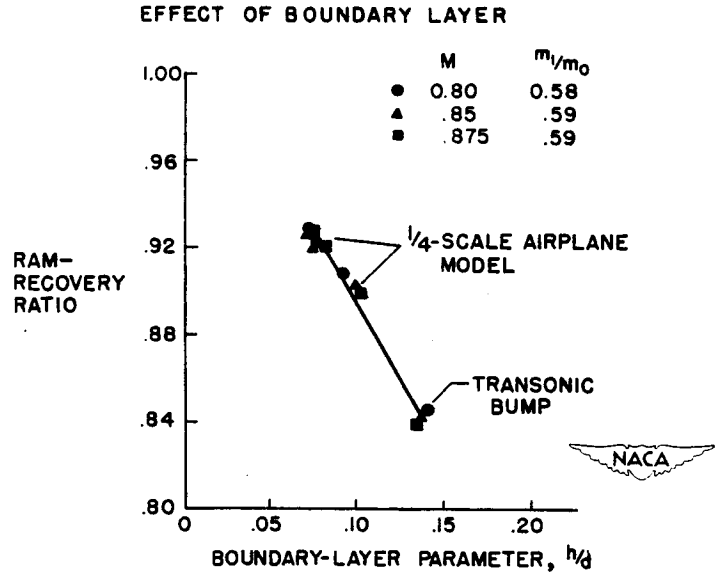

Figure 4.- Effect of boundary layer on the pressure recovery of NACA submerged inlets.

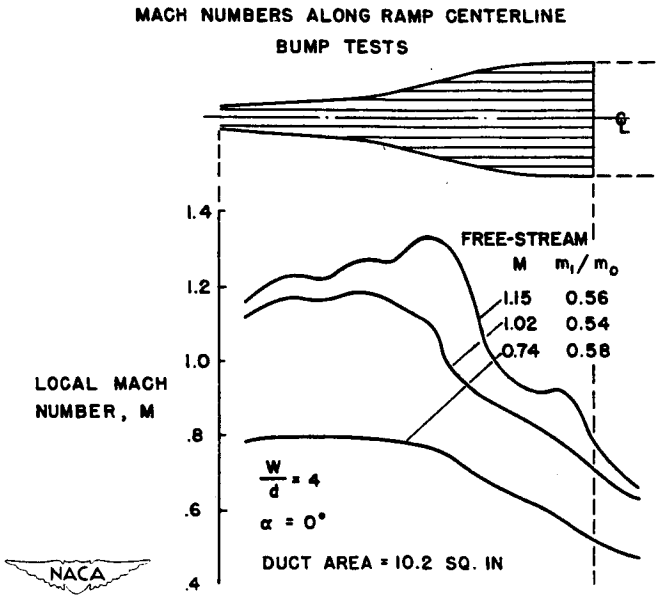

Figure 5.- Mach number distribution along the ramp center line from the transonic-bump tests of an NACA submerged inlet.

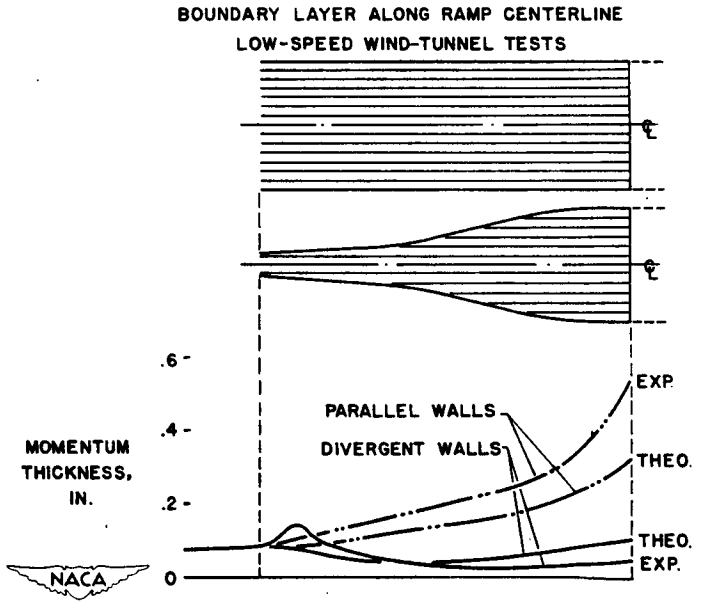

Figure 6.- Comparison of the experimental and theoretical boundary-layer growth along the ramps of submerged inlets.

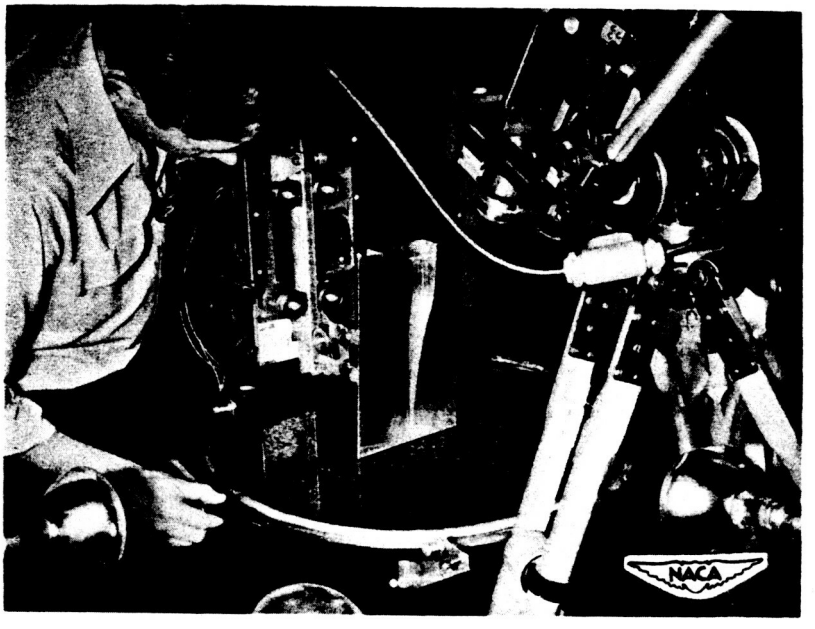

Figure 7.- Water-flow study apparatus.

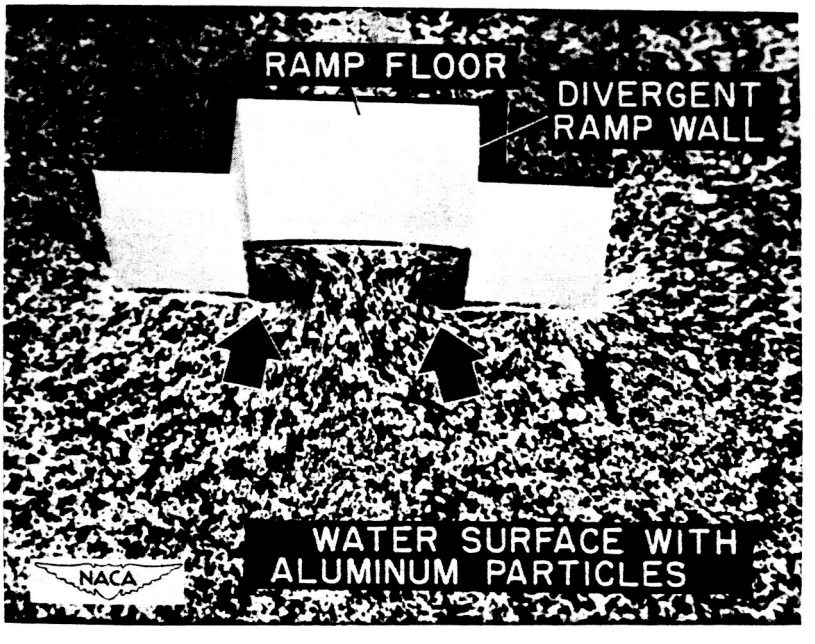

Figure 8.- Vortex formed in an NACA submerged inlet.

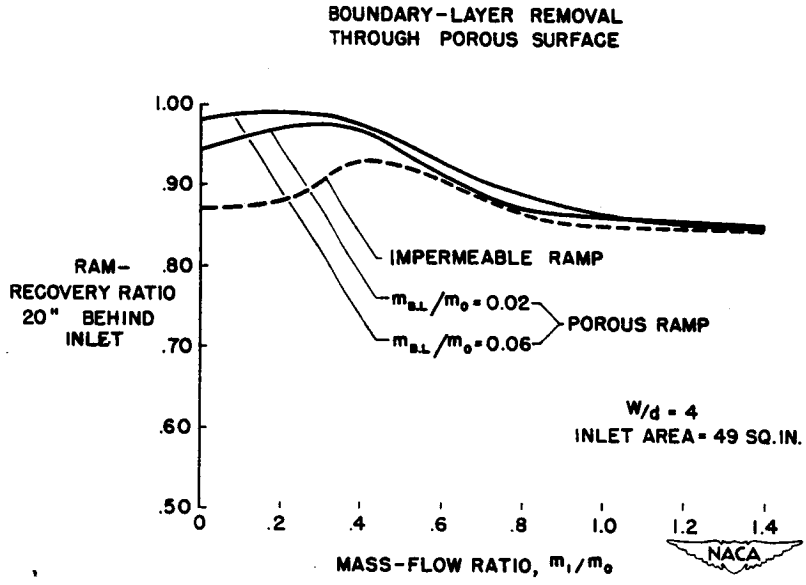

Figure 9.- Effect of boundary-layer removal through a porous ramp on the pressure recovery of an NACA submerged inlet.